Interaction of Melittin with Membrane Cholesterol: A Fluorescence Approach

H. Raghuraman and Amitabha Chattopadhyay
Centre for Cellular and Molecular Biology, Hyderabad 500 007, India

ABSTRACT We have monitored the organization and dynamics of the hemolytic peptide melittin in membranes containing cholesterol by utilizing the intrinsic fluorescence properties of its functionally important sole tryptophan residue and circular dichroism spectroscopy. The significance of this study is based on the fact that the natural target for melittin is the erythrocyte membrane, which contains high amounts of cholesterol. Our results show that the presence of cholesterol inhibits melittin-induced leakage of lipid vesicles and the extent of inhibition appears to be dependent on the concentration of membrane cholesterol. The presence of cholesterol is also shown to reduce binding of melittin to membranes. Our results show that fluorescence parameters such as intensity, emission maximum, and lifetime of membrane-bound melittin indicate a change in polarity in the immediate vicinity of the tryptophan residue probably due to increased water penetration in presence of cholesterol. This is supported by results from fluorescence quenching experiments using acrylamide as the quencher. Membrane penetration depth analysis by the parallax method shows that the melittin tryptophan is localized at a relatively shallow depth in membranes containing cholesterol. Analysis of energy transfer results using melittin tryptophan (donor) and dehydroergosterol (acceptor) indicates that dehydroergosterol is not randomly distributed and is preferentially localized around the tryptophan residue of membrane-bound melittin, even at the low concentrations used. Taken together, our results are relevant in understanding the interaction of melittin with membranes in general, and with cholesterol-containing membranes in particular, with possible relevance to its interaction with the erythrocyte membrane.

INTRODUCTION

Although cell lysis by toxic peptides has been extensively studied, the molecular mechanism of lysis is still not well understood. A particularly interesting and popular lytic peptide is melittin, which is the major toxic component in the venom of the European honey bee, *Apis mellifera*. It is a small linear peptide composed of 26 amino acid residues (NH_2-GIGAVLKVLTTGLPALISWIKRKRQQ-$CONH_2$) and is known to have a powerful hemolytic activity (Dempsey, 1990). It is a cationic peptide in which the amino terminal is composed predominantly of hydrophobic amino acids (residues 1–20), whereas the carboxy terminal end has a stretch of predominantly hydrophilic amino acids (residues 21–26) that give rise to its amphiphilic character. This amphiphilic property of melittin makes it water soluble and yet it spontaneously associates with natural and artificial membranes (Dempsey, 1990; Saberwal and Nagaraj, 1994). Such a sequence of amino acids, coupled with its amphiphilic nature, is characteristic of many membrane-bound peptides and putative transmembrane helices of membrane proteins (Dempsey, 1990). This has resulted in melittin being used as a convenient model to monitor lipid-protein interactions in membranes.

Despite the availability of a high-resolution (2-Å) crystal structure of tetrameric melittin in aqueous solution (Terwilliger and Eisenberg, 1982), the structure of the membrane-bound form is not yet resolved by x-ray crystallography. Because the association of the peptide in the membrane is linked to its physiological effects (Dempsey, 1990), a detailed understanding of the interaction of melittin with membrane components assumes significance. The importance of the membrane-bound form also stems from the observation that the amphiphilic α-helical conformation of this hemolytic toxin in membranes resembles those of signal peptides (Golding and O'Shea, 1995), and the envelope glycoprotein gp41 from the human immunodeficiency virus (HIV) (Rabenstein and Shin, 1995). Furthermore, understanding melittin-membrane interaction assumes greater significance due to the recent finding that melittin mimics the N-terminal of HIV-1 virulence factor Nef1-25 (Barnham et al., 1997). Interestingly, it has been recently shown that the Nef protein associates with membrane microdomains (rafts), in which a major component is cholesterol (Wang et al., 2000). However, despite a number of studies, there appears to be no consensus regarding the orientation, depth of penetration into the membrane, and aggregation state of membrane-bound melittin (Dempsey, 1990).

Melittin is intrinsically fluorescent due to the presence of a single tryptophan residue, Trp-19, which makes it a sensitive probe to study the interaction of melittin with membranes and membrane-mimetic systems (Ghosh et al., 1997; Bradrick et al., 1995; Raghuraman and Chattopadhyay, 2003, 2004). This is particularly advantageous because there are no other aromatic amino acids in melittin and this makes interpretation of fluorescence data less complicated due to lack of interference and heterogeneity. More importantly, it has been shown

Submitted March 26, 2004, and accepted for publication June 28, 2004.

Address reprint requests to Amitabha Chattopadhyay, Centre for Cellular and Molecular Biology, Uppal Road, Hyderabad 500 007, India. Tel.: 91-40-2719-2578; Fax: 91-40-2716-0311; E-mail: amit@ccmb.res.in.

0006-3495/04/10/2419/14 $2.00

doi: 10.1529/biophysj.104.043596

that the sole tryptophan residue of melittin is crucial for its powerful hemolytic activity because a dramatic reduction in activity is observed upon photooxidation (Habermann and Kowallek, 1970), and substitution by leucine (Blondelle and Houghten, 1991a). This is further reinforced by studies with single amino acid omission analogs of melittin (Blondelle and Houghten, 1991b). These reports point out the crucial role played by the uniquely positioned tryptophan in maintaining the structure and hemolytic activity of melittin. The organization and dynamics of the tryptophan therefore become important for the function of the peptide. We have previously monitored the microenvironment experienced by the sole tryptophan in melittin when bound to membranes utilizing the wavelength-selective fluorescence approach. Our results show that the tryptophan residue is located in a motionally restricted region in the membrane (Ghosh et al., 1997; Chattopadhyay and Rukmini, 1993) and the tryptophan environment is modulated by the surface charge of the membrane, which could be related to the difference in the lytic activity of the peptide observed in membranes of varying charge (Ghosh et al., 1997).

Cholesterol is an essential component of eukaryotic membranes and plays a crucial role in membrane organization, dynamics, function, and sorting (Simons and Ikonen, 2000; Yeagle, 1985). It is often found distributed nonrandomly in domains or pools in biological and model membranes (Simons and Ikonen, 2000, 1997; Yeagle, 1985; Mukherjee and Chattopadhyay, 1996; Rukmini et al., 2001). Many of these domains are believed to be important for the maintenance of membrane structure and function. Recent observations suggest that cholesterol exerts many of its actions by maintaining a specialized type of membrane domain, termed ''lipid raft,'' in a functional state (Simons and Ikonen, 1997) although the existence of lipid rafts in membranes has not been unequivocally shown (Munro, 2003). In view of the importance of cholesterol in relation to membrane domains, the interaction of cholesterol with membrane proteins (Yeagle, 1985) represents an important determinant in functional studies of such proteins.

It has been proposed that the rigid ring system and perpendicular orientation in relation to the plane of the membrane make cholesterol an attractive target for many bacterial toxins and fungal antibiotics (de Kruijff, 1990). In addition, it has been suggested that the tryptophans in the toxins could potentially form a stable complex with the rigid ring system of the cholesterol molecule. In this article, we report the effect of cholesterol on the organization and dynamics of melittin utilizing a combination of spectroscopic approaches that include the wavelength-selective fluorescence approach, resonance energy transfer, and circular dichroism (CD) spectroscopy. The functional significance of the interaction of melittin with membrane cholesterol is brought out by the fact that the presence of cholesterol in the membrane inhibits the lytic activity of melittin (Benachir et al., 1997). Interestingly, the natural target for melittin is the erythrocyte membrane that contains high amounts of cholesterol (Yeagle, 1985). The organization and dynamics of the sole tryptophan residue of melittin, which has been earlier shown to be crucial for its hemolytic activity (Habermann and Kowallek, 1970; Blondelle and Houghten, 1991a,b), therefore become an important issue in cholesterol-containing membranes.

MATERIALS AND METHODS

Materials

Melittin, calcein, $\Delta^{5,7,9(11)22}$-ergostatetraen-3β-ol, or dehydroergosterol (DHE), L-tryptophan, *N*-acetyl-L-tryptophanamide (NATA), 1,2-dimyristoyl-*sn*-glycero-3-phosphocholine (DMPC), and 3-(*N*-morpholino)propanesulfonic acid (MOPS) were obtained from Sigma Chemical (St. Louis, MO). 1,2-Dioleoyl-*sn*-glycero-3-phosphocholine (DOPC), 1-palmitoyl-2-(5-doxyl)stearoyl-*sn*-glycero-3-phosphocholine (5-PC), and 1-palmitoyl-2-(12-doxyl)stearoyl-*sn*-glycero-3-phosphocholine (12-PC) were purchased from Avanti Polar Lipids (Alabaster, AL). Anthroyloxy-labeled fatty acids such as 2-(9-anthroyloxy)stearic acid (2-AS) and 12-(9-anthroyloxy)stearic acid (12-AS) were from Molecular Probes (Eugene, OR). To check for any residual phospholipase A_2 contamination in melittin, phospholipase activity was assayed using ^{14}C-labeled (DOPC) (Amersham International, Buckinghamshire, UK) as described earlier (Ghosh et al., 1997). Lipids were checked for purity by thin layer chromatography on silica gel precoated plates (Sigma) in chloroform/methanol/water (65:35:5, v/v/v) and were found to give only one spot in all cases with a phosphate-sensitive spray and on subsequent charring (Dittmer and Lester, 1964). The concentration of DOPC was determined by phosphate assay subsequent to total digestion by perchloric acid (McClare, 1971). DMPC was used as an internal standard to assess lipid digestion. The concentration of melittin in aqueous solution was calculated from its molar extinction coefficient (ε) of 5570 $M^{-1}cm^{-1}$ at 280 nm (Ghosh et al., 1997). Ultrapure-grade acrylamide was from Gibco BRL (Rockville, MD). The purity of acrylamide was checked from its absorbance using its molar extinction coefficient (ε) of 0.23 $M^{-1}cm^{-1}$ at 295 nm and optical transparency beyond 310 nm (Eftink, 1991a). All other chemicals used were of the highest purity available. Solvents used were of spectroscopic grade. Water was purified through a Millipore (Bedford, MA) Milli-Q system and used throughout.

Sample preparations

Small unilamellar vesicles of DOPC containing increasing concentrations (0–40 mol%) of cholesterol and 0.5 mol% melittin (1 mol% for energy transfer and CD measurements) were prepared. The vesicles were prepared by drying 2560 nmol (1280 nmol for energy transfer experiments) of total lipid (DOPC or DOPC/cholesterol) under a stream of nitrogen while being warmed gently (35°C) and then under a high vacuum for at least 3 h. The lipids were swollen by adding 1.5 ml of 10 mM MOPS, 150 mM NaCl, pH 7.2 buffer containing 5 mM EDTA (to suppress any residual phospholipase A_2 activity), and vortexed for 3 min to disperse the lipid. The lipid dispersions were then sonicated under argon until they were clear using a bath sonicator (Laboratory Supplies, Hicksville, NY). To incorporate melittin into membranes, a small aliquot containing 12.8 nmol (25.6 nmol for CD measurements) of melittin was added from a stock solution in water to the preformed vesicles and mixed well. For acrylamide quenching experiments, the total lipid used was less to avoid scattering artifacts. For these experiments, 320 nmol of total lipid (DOPC or DOPC/cholesterol) was used to prepare vesicles as mentioned above and melittin was incorporated into membranes by adding a small aliquot containing 1.6 nmol of melittin from a stock solution in water to the preformed vesicles and mixed well to give membranes containing 0.5 mol% melittin. Samples were kept in the

dark for 12 h before measuring fluorescence. Background samples were prepared the same way except that melittin was not added to them. All experiments were done at room temperature (23°C).

Depth measurements using the parallax method

The actual spin (nitroxide) content of the spin-labeled phospholipids (5- and 12-PC) was assayed using fluorescence quenching of anthroyloxy-labeled fatty acids (2- and 12-AS) as described earlier (Abrams and London, 1993). For depth measurements, liposomes were made by the ethanol injection method (Kremer et al., 1977). These samples were made by drying 640 nmol of total lipid (DOPC or DOPC/cholesterol) containing 15 mol% spin-labeled phospholipid (5- or 12-PC) under a stream of nitrogen while being warmed gently (35°C) followed by further drying under a high vacuum for at least 3 h. The dried lipid film was dissolved in ethanol to give a final concentration of 40 mM. The ethanolic lipid solution was then injected into 10 mM MOPS, 150 mM NaCl, pH 7.2 buffer containing 5 mM EDTA, while vortexing to give a final concentration of 0.43 mM total lipid in the buffer. Melittin was incorporated into membranes by adding a small aliquot containing 3.2 nmol of melittin from a stock solution in water to the preformed vesicles and mixed well to give membranes containing 0.5% melittin. The lipid composition of these samples were as follows: i), DOPC (85%) and 5- or 12-PC (15%); ii), DOPC (65%), 5- or 12-PC (15%), and cholesterol (20%); and iii), DOPC (45%), 5- or 12-PC (15%) and cholesterol (40%). Duplicate samples were prepared in each case except for samples lacking the quencher (5- or 12-PC) where triplicates were prepared. Background samples lacking the fluorophore (melittin) were prepared in all experiments, and their fluorescence intensity was subtracted from the respective sample fluorescence intensity. Samples were kept in the dark for 12 h before measuring fluorescence.

Steady-state fluorescence measurements

Steady-state fluorescence measurements were performed with a Hitachi F-4010 spectrofluorometer (Hitachi, Tokyo, Japan) using 1-cm pathlength quartz cuvettes. Excitation and emission slits with a nominal bandpass of 5 nm were used for all measurements unless mentioned otherwise. All spectra were recorded using the correct spectrum mode. Background intensities of samples in which melittin was omitted were subtracted from each sample spectrum to cancel out any contribution due to the solvent Raman peak and other scattering artifacts. Fluorescence polarization measurements were performed at room temperature (23°C) using a Hitachi polarization accessory. Polarization values were calculated from the equation (Lakowicz, 1999):

$$P = \frac{I_{VV} - GI_{VH}}{I_{VV} + GI_{VH}}, \tag{1}$$

where I_{VV} and I_{VH} are the measured fluorescence intensities (after appropriate background subtraction) with the excitation polarizer vertically oriented and emission polarizer vertically and horizontally oriented, respectively. G is the grating correction factor and is the ratio of the efficiencies of the detection system for vertically and horizontally polarized light, and is equal to I_{HV}/I_{HH}. All experiments were done with multiple sets of samples and average values of polarization are shown in Table 1. The spectral shifts obtained with different sets of samples were identical in most cases. In other cases, the values were within ±1 nm of the ones reported.

For depth measurements, samples were excited at 280 nm and emission was collected at 336 nm. Excitation and emission slits with a nominal bandpass of 5 nm were used. Fluorescence was measured at room temperature and averaged over two 5-s readings. Intensities were found to be stable over time. In all cases, the intensity from background samples without fluorophore was subtracted. Membrane penetration depths were calculated using Eq. 10 (see Results).

TABLE 1 Fluorescence emission characteristics of melittin in DOPC membranes containing cholesterol

Cholesterol (mol%)	Fluorescence emission maximum (nm)	REES (nm)	Fluorescence polarization*
0	336	6	0.132 ± 0.001
10	336	6	0.133 ± 0.002
20	337	6	0.132 ± 0.001
30	337	5	0.133 ± 0.002
40	338	5	0.127 ± 0.001

*Calculated using Eq. 1. The polarization value represents mean ± SE of at least three independent measurements. The ratio of melittin/total lipid was 1:200 (mol/mol) and the concentration of melittin was 8.53 μM. See Materials and Methods for other details.

Time-resolved fluorescence measurements

Fluorescence lifetimes were calculated from time-resolved fluorescence intensity decays using a Photon Technology International (London, Western Ontario, Canada) LS-100 luminescence spectrophotometer in the time-correlated single-photon counting mode as described previously (Raghuraman and Chattopadhyay, 2003). All experiments were performed using slits with a nominal bandpass of 4 nm or less. Fluorescence intensity decay curves obtained were deconvoluted with the instrument response function and analyzed as a sum of exponential terms:

$$F(t) = \sum_i \alpha_i \exp(-t/\tau_i), \tag{2}$$

where $F(t)$ is the fluorescence intensity at time t and α_i is a preexponential factor representing the fractional contribution to the time-resolved decay of the component with a lifetime τ_i such that $\sum_i \alpha_i = 1$. The decay parameters were recovered as described previously (Raghuraman and Chattopadhyay, 2003). Mean (average) lifetimes $\langle\tau\rangle$ for biexponential decays of fluorescence were calculated from the decay times and preexponential factors using the following equation (Lakowicz, 1999):

$$\langle\tau\rangle = \frac{\alpha_1\tau_1^2 + \alpha_2\tau_2^2}{\alpha_1\tau_1 + \alpha_2\tau_2}. \tag{3}$$

Acrylamide quenching measurements

Acrylamide quenching experiments in membranes of various concentrations of cholesterol were carried out by measurement of fluorescence intensity of melittin in separate samples containing increasing concentrations of acrylamide taken from a freshly prepared stock solution (8 M) in water. Samples were kept in dark for 1 h before measuring fluorescence. The excitation wavelength used was 295 nm and emission was monitored at the fluorescence emission maximum of melittin in the given membrane system. Corrections for inner filter effect were made using the following equation (Lakowicz, 1999):

$$F = F_{obs}\,\text{antilog}[(A_{ex} + A_{em})/2], \tag{4}$$

where F is the corrected fluorescence intensity and F_{obs} is the background subtracted fluorescence intensity of the sample. A_{ex} and A_{em} are the measured absorbance at the excitation and emission wavelengths. The

absorbance of the samples was measured using a Hitachi U-2000 ultraviolet (UV)-visible absorption spectrophotometer. Quenching data were analyzed by fitting to the Stern-Volmer equation (Lakowicz, 1999):

$$F_o/F = 1 + K_{SV}[Q] = 1 + k_q\tau_o[Q], \quad (5)$$

where F_o and F are the fluorescence intensities in the absence and presence of the quencher, respectively, $[Q]$ is the molar quencher concentration and K_{SV} is the Stern-Volmer quenching constant. The Stern-Volmer quenching constant K_{SV} is equal to $k_q\tau_o$ where k_q is the bimolecular quenching constant and τ_o is the lifetime of the fluorophore in the absence of quencher.

Energy transfer measurements

All experiments were done using small unilamellar vesicles (SUVs) containing 1280 nmol of DOPC with varying amounts of DHE (0–4 mol%) and 1 mol% of melittin. The tryptophan residue of melittin served as the donor whereas DHE was used as the acceptor. The energy transfer efficiencies were calculated using the equation (Lakowicz, 1999):

$$E = (1 - F/F_o), \quad (6)$$

where E is the efficiency of energy transfer and F and F_o are fluorescence intensities of the donor (tryptophan of melittin) in the presence and absence of the acceptor (DHE), respectively. The quantum yield (Q_D) of membrane-bound melittin was determined using the equation (Parker and Rees, 1960):

$$Q_D = Q_S(F_D/F_S)(A_S/A_D)(n_D^2/n_S^2), \quad (7)$$

where the subscripts ''S'' and ''D'' refer to the reference standard and the donor, respectively. F is the wavenumber-integrated area of the corrected emission at constant slit openings, A is the absorbance at the excitation wavelength (<0.1 to avoid inner filter effect); and n is the refractive index of the medium in which the standard or the sample is placed. Both L-tryptophan ($Q_S = 0.13$ in water; Lakowicz, 1999) and NATA ($Q_S = 0.14$ in water; Szabo and Rayner, 1980) were used as reference standards and the internal consistency of the results was checked by measuring the quantum yield of one standard with respect to the other. Solutions were freshly prepared and degassed by bubbling high-purity nitrogen before use. Refractive index was measured using a DUR refractometer (Schmidt-Haensch, Germany).

Circular dichroism measurements

CD measurements were carried out at room temperature (23°C) in a JASCO J-715 spectropolarimeter, which was calibrated with (+)-10-camphorsulfonic acid. The spectra were scanned in a quartz optical cell with a pathlength of 0.1 cm. All spectra were recorded in 0.2-nm wavelength increments with a 4-s response and a band width of 1 nm. For monitoring changes in secondary structure, spectra were scanned in the far-UV range from 205 to 250 nm at a scan rate of 50 nm/min. Each spectrum is the average of 15 scans with a full-scale sensitivity of 50 mdeg. All spectra were corrected for background by subtraction of appropriate blanks and were smoothed making sure that the overall shape of the spectrum remains unaltered. Data are represented as mean residue ellipticities and were calculated using the equation:

$$[\theta] = \theta_{obs}/(10Cl), \quad (8)$$

where θ_{obs} is the observed ellipticity in mdeg, l is the pathlength in cm, and C is the concentration of peptide bonds in mol/L.

Assay for the permeabilization of lipid vesicles

The ability of melittin to cause release of entrapped vesicle contents for SUVs composed of varying amounts of cholesterol was checked by monitoring the increase in fluorescence intensity of calcein, encapsulated in vesicles at high self-quenching concentrations (70 mM), upon addition of melittin (Allen, 1984). Calcein-loaded liposomes were separated from nonencapsulated (free) calcein by gel filtration on a Sephadex G-75 column (Sigma) using an elution buffer of 10 mM MOPS, 150 mM NaCl and 5 mM EDTA (pH 7.4), and lipid concentrations were estimated by complexation with ammonium ferrothiocyanate (Stewart, 1980). Fluorescence was measured at room temperature (23°C) in a Hitachi F-4010 spectrofluorometer using 1-cm pathlength cuvettes. The excitation wavelength was 490 nm and emission was set at 520 nm. Excitation and emission slits with a nominal bandpass of 3 and 5 nm were used, respectively. The high concentration (70 mM) of the entrapped calcein led to self-quenching of its fluorescence resulting in low fluorescence intensity of the vesicles (I_B). An aliquot of melittin solution in water was then added and mixed properly to obtain the desired peptide to lipid ratio. Release of calcein caused by addition of melittin led to the dilution of the dye into the medium, which could therefore be monitored by an enhancement of fluorescence intensity (I_F). This enhancement of fluorescence is a measure of the extent of vesicle permeabilization. Fluorescence was continuously monitored after the addition of melittin to the vesicles. The experiments were normalized relative to the total fluorescence intensity (I_T) corresponding to the total release of calcein after complete disruption of all the vesicles by addition of Triton X-100 (2% v/v). Calcein release could not be detected with vesicles alone (without any addition of melittin) in the timescale of the experiment. The percentage of calcein release in the presence of melittin was calculated using the equation (Benachir et al., 1997):

$$\% \text{ release} = 100(I_F - I_B)/(I_T - I_B), \quad (9)$$

where I_B is the background (self-quenched) intensity of calcein encapsulated in vesicles, I_F represents the enhanced fluorescence intensity resulting from the dilution of dye in the medium caused by melittin-induced release of entrapped calcein. I_T is the total fluorescence intensity after complete permeabilization is achieved upon addition of Triton X-100.

RESULTS

Cholesterol inhibits melittin-induced lysis

The effect of cholesterol on the lytic activity of melittin is shown in Fig. 1. Because cholesterol modifies the physical properties of the bilayer (Yeagle, 1985), we examined whether these changes influence the lytic ability of melittin. The percentage of calcein release was calculated according to Eq. 9 and is shown in Fig. 1. As is apparent from the figure, the lytic efficiency of melittin increases with increasing peptide concentration, i.e., with decreasing lipid/peptide ratio (mol/mol) in all cases, irrespective of the presence of cholesterol in the membrane. More importantly, the lytic efficiencies of melittin appear to be dependent on the composition of the membrane. Our results show that the presence of cholesterol in the membrane inhibits the lytic power of melittin and the inhibition is enhanced with increasing cholesterol concentration. This is in agreement with earlier results in which it was shown that the presence of cholesterol inhibits melittin-induced lysis (Benachir et al., 1997).

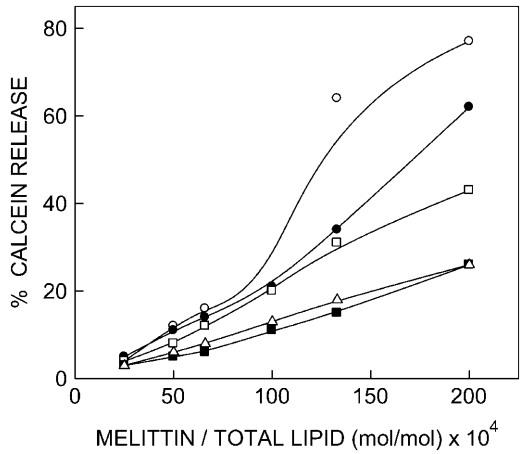

FIGURE 1 Release of entrapped calcein as a function of melittin/lipid (mol/mol) ratio in DOPC vesicles containing 0 (○), 10 (●), 20 (□), 30 (■), and 40 (△) mol% cholesterol. Lipid concentration used was 41.9 μM. See Materials and Methods for other details.

Binding of melittin to membranes containing cholesterol

Because the presence of cholesterol in the membrane could affect the binding (and hence lytic activity) of melittin to membranes, we monitored the binding of melittin to DOPC membranes containing varying amounts of cholesterol utilizing the intrinsic fluorescence of the sole tryptophan residue in melittin. The binding of melittin to membranes can be quantitated by the blue shift of emission maximum (from 352 to 336 nm) upon binding to the lipid vesicles, which is due to the change in the polarity of the surrounding medium because melittin in buffer exhibits an emission maximum at 352 nm. The increase in fluorescence intensity ratio (F_{336}/F_{352}) therefore represents the fraction of membrane-bound melittin. Fig. 2 *a* shows the binding curve for melittin binding to DOPC vesicles monitored this way. Binding of melittin to DOPC vesicles is efficient and reaches a plateau at a lipid/peptide ratio of ~50 (mol/mol), and becomes less efficient with incorporation of increasing amounts of cholesterol in the membrane. Thus, with DOPC vesicles containing 40 mol% cholesterol, complete binding of melittin is only achieved at a lipid/peptide ratio of ~200 (mol/mol). This suggests that the presence of cholesterol reduces the binding of melittin to DOPC vesicles. This is further supported by measurements of fluorescence polarization as a function of increasing lipid/melittin ratio (mol/mol) (see Fig. 2 *b*). We therefore chose conditions for our experiments in such a way so as to ensure that melittin is predominantly membrane bound, i.e., there is no ground state heterogeneity.

Fluorescence of membrane-bound melittin

The fluorescence emission spectra of melittin in DOPC vesicles containing different amounts of cholesterol are shown in Fig. 3 *a*. The maximum of fluorescence emission

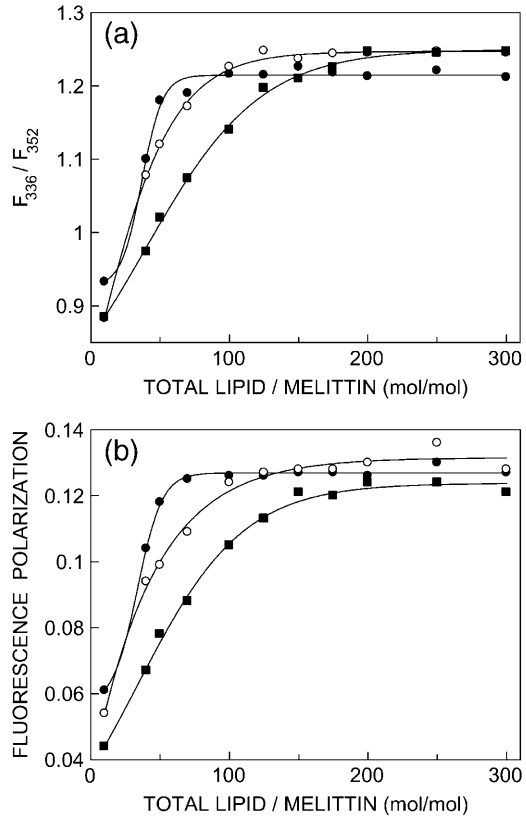

FIGURE 2 Binding of melittin to DOPC vesicles containing different amounts of cholesterol measured by changes in melittin fluorescence: *a*), the ratio of fluorescence intensity monitored at 336 and 352 nm; and b), fluorescence polarization plotted as a function of total lipid/melittin ratio (mol/mol) for vesicles containing 0 (●), 10 (○), and 40 (■) mol% cholesterol. The excitation wavelength used was 280 nm and fluorescence polarization was monitored at 336 nm. The concentration of melittin was 4.26 μM in all cases. See Materials and Methods for other details.

of melittin in DOPC vesicles is 336 nm, as has been reported previously (Ghosh et al., 1997). We have used the term maximum of fluorescence emission in a somewhat wider sense here. In every case, we have monitored the wavelength corresponding to maximum fluorescence intensity, as well as the center of mass of the fluorescence emission. In most cases, both these methods yielded the same wavelength. In cases where minor discrepancies were found, the center of mass of emission has been reported as the fluorescence maximum. The fluorescence emission maximum is slightly shifted toward longer wavelength (338 nm) in the presence of high amounts (40 mol%) of cholesterol (see Table 1). This is accompanied by a marked reduction (36%) in peak fluorescence intensity (see Fig. 3 *b*). The reduction in fluorescence intensity could possibly be due to both specific and general bilayer effects induced by cholesterol. The specific effect could be due to the close proximity of cholesterol to melittin tryptophan that could imply specific interaction between melittin and cholesterol. On the other hand, tryptophan fluorescence intensity is known to be sensitive to the presence of water in its immediate

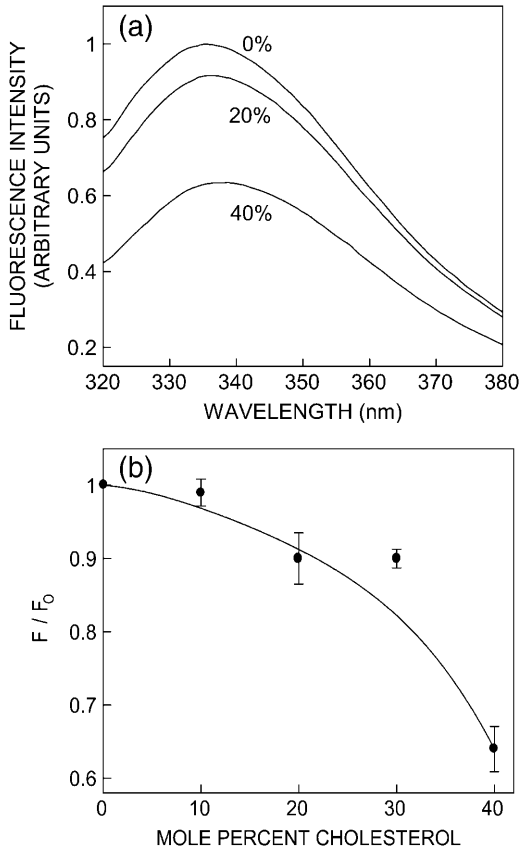

FIGURE 3 Effect of increasing amounts of cholesterol on fluorescence emission spectra and intensity of membrane-bound melittin: *a*), representative fluorescence emission spectra of melittin in DOPC vesicles containing 0, 20, and 40 mol% cholesterol; and *b*), fluorescence intensity of membrane-bound melittin as a function of cholesterol concentration. The data points shown are the means of at least three independent measurements. The error bars represent the standard error. The ratio of melittin/total lipid was 1:200 (mol/mol) and the concentration of melittin was 8.53 μM in all cases. The excitation wavelength used was 280 nm in all cases and emission was monitored at 336 nm in panel *b*. See Materials and Methods for other details.

environment (Ladokhin, 2000). The decrease in the fluorescence intensity as well as the red shift of the emission maximum could therefore be due to increased water penetration in the interfacial region (where the tryptophan residue in membrane-bound melittin is localized; Ghosh et al., 1997) of the membrane induced by cholesterol (Subczynski et al., 1994). Control experiments with tryptophan octyl ester, a model tryptophan analog for membrane-bound tryptophans characterized by an interfacially localized tryptophan (Chattopadhyay et al., 1997), showed that reduction in fluorescence intensity observed with membrane-bound melittin is not solely due to general bilayer effects (not shown).

Red-edge excitation shift and fluorescence polarization of membrane-bound melittin

Red-edge excitation shift (REES) represents a powerful approach that can be used to directly monitor the environment and dynamics around a fluorophore in a complex biological system (Chattopadhyay, 2003; Raghuraman et al., 2003). A shift in the wavelength of maximum fluorescence emission toward higher wavelengths, caused by a shift in the excitation wavelength toward the red edge of the absorption band, is termed REES. This effect is mostly observed with polar fluorophores in motionally restricted media such as viscous solutions or condensed phases where the dipolar relaxation time for the solvent shell around a fluorophore is comparable to or longer than its fluorescence lifetime (Chattopadhyay, 2003; Raghuraman et al., 2003; Demchenko, 2002). We have previously shown that REES serves as a powerful tool to monitor the organization and dynamics of fluorescent probes and peptides/proteins bound to membranes and membrane-mimetic media such as micelles and reverse micelles (Chattopadhyay, 2003 and references therein; Kelkar et al., 2003; Mukherjee et al., 2004; Raghuraman et al., 2004; Raghuraman and Chattopadhyay, 2003, 2004; Rawat et al., 2004).

The magnitude of REES of the tryptophan residue of membrane-bound melittin with increasing amounts of cholesterol is shown in Table 1. As the excitation wavelength is changed from 280 to 307 nm, the maximum of emission wavelength of the melittin tryptophan is shifted from 336 to 342 nm in case of vesicles containing only DOPC and DOPC/10 mol% cholesterol, and from 337 to 343 nm for DOPC vesicles containing 20 mol% cholesterol. In all these cases, the magnitude of REES corresponds to 6 nm. Such dependence of the emission maximum on excitation wavelength is characteristic of REES. This implies that the tryptophan residue in melittin is localized in a motionally restricted region of the membrane in these cases. This is consistent with the interfacial localization of the melittin tryptophan when bound to membranes (Ghosh et al., 1997; Chattopadhyay and Rukmini, 1993). Interestingly, the magnitude of REES does not appear to be critically dependent on the cholesterol content of the membrane (see Table 1).

The steady-state fluorescence polarization of melittin in DOPC vesicles containing increasing amounts of cholesterol is shown in Table 1. These values are representative of motionally restricted tryptophan environments (Ghosh et al., 1997; Chattopadhyay and Rukmini, 1993) and do not change with increasing cholesterol concentrations up to 30 mol%. A small (~4%) reduction in polarization is observed in DOPC vesicles containing 40 mol% cholesterol, probably due to change in headgroup packing induced by cholesterol (Yeagle, 1985), which could increase the rotational mobility of the tryptophan residue. In addition, fluorescence polarization is also known to be dependent on excitation and emission wavelengths in motionally restricted media (Mukherjee and Chattopadhyay, 1995). We measured polarization changes of melittin bound to DOPC and DOPC/cholesterol vesicles as a function of excitation and emission wavelengths. Our results show that membrane-bound melittin exhibits wavelength-dependent changes in polarization for both excitation and

emission (data not shown). This reinforces that melittin is localized in a motionally restricted interfacial region of the membrane in these cases.

Time-resolved fluorescence measurements of membrane-bound melittin

It is well known that fluorescence lifetime of tryptophan in particular is sensitive to solvent, temperature, and excited-state interactions (Kirby and Steiner, 1970). A typical decay profile of tryptophan residue of membrane-bound melittin with its biexponential fitting and the statistical parameters used to check the goodness of the fit is shown in Fig. 4.

The fluorescence lifetimes of melittin bound to membranes containing varying amounts of cholesterol are shown in Table 2. As seen from the table, all fluorescence decays could be fitted well with a biexponential function. The mean fluorescence lifetimes were calculated using Eq. 3 and are shown in Fig. 5. As shown in the figure, there is a progressive decrease (amounting to ~20% in case of DOPC vesicles containing 40 mol% cholesterol) in the mean fluorescence lifetime of the tryptophan residue of membrane-bound melittin with increasing cholesterol concentrations. In general, an increase in polarity of the tryptophan environment is known to reduce the lifetime of tryptophans due to fast deactivating processes in polar environments (Kirby and Steiner, 1970). The decrease

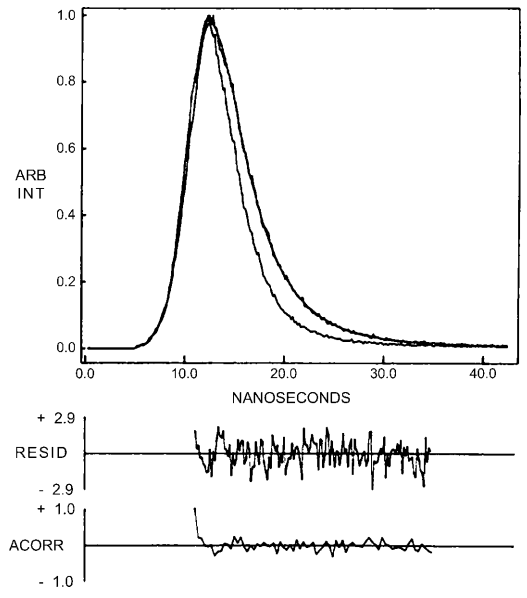

FIGURE 4 Time-resolved fluorescence intensity decay of melittin in DOPC vesicles. Excitation wavelength was 297 nm, which corresponds to a peak in the spectral output of the nitrogen lamp. Emission was monitored at 336 nm. The sharp peak on the left is the lamp profile. The relatively broad peak on the right is the decay profile, fitted to a biexponential function. The two lower plots show the weighted residuals and the autocorrelated function of the weighted residuals. The ratio of melittin/total lipid was 1:200 (mol/mol) and the concentration of melittin was 8.53 μM in all cases. See Materials and Methods for other details.

TABLE 2 Fluorescence lifetimes of melittin in DOPC membranes containing cholesterol

Cholesterol (mol%)	α_1	τ_1 (ns)	α_2	τ_2 (ns)
0	0.89	0.64	0.11	3.24
10	0.92	0.67	0.08	3.48
20	0.92	0.83	0.08	3.54
30	0.90	0.64	0.10	3.08
40	0.92	0.60	0.08	2.99

The excitation wavelength was 297 nm; emission was monitored at 336 nm. The ratio of melittin/total lipid was 1:200 (mol/mol) and the concentration of melittin was 8.53 μM. See Materials and Methods for other details.

in the fluorescence lifetime could therefore possibly be due to increased water penetration in the interfacial region of the membrane induced by cholesterol (Subczynski et al., 1994; Stubbs et al., 1995). This is consistent with our earlier observation of reduction in fluorescence intensity of membrane-bound melittin with increasing amounts of cholesterol in the membrane (see Fig. 3).

Acrylamide quenching of melittin tryptophan fluorescence

Acrylamide quenching of tryptophan fluorescence is widely used to monitor tryptophan environments in proteins and peptides (Eftink, 1991b). The slope of the Stern-Volmer plot, obtained from acrylamide quenching experiments, is the Stern-Volmer constant (K_{SV}). This parameter (K_{SV}) is related to the degree of exposure (accessibility) of the melittin tryptophan to the water soluble quencher. In general, the higher the slope, the greater the degree of exposure, assuming that there is not a large difference in fluorescence lifetime. The quenching parameter (K_{SV}) obtained by analyzing the Stern-Volmer plots is shown in Table 3. The

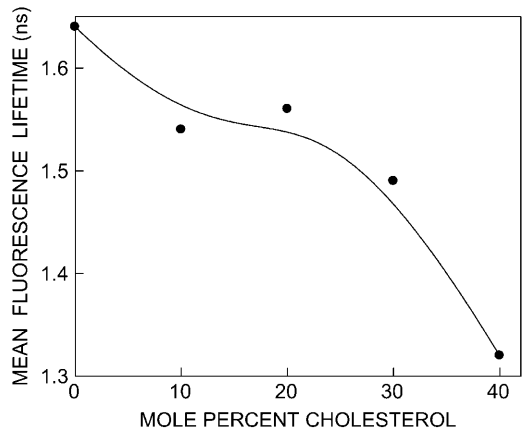

FIGURE 5 Mean fluorescence lifetime of melittin in DOPC vesicles containing increasing concentration of cholesterol. The excitation wavelength used was 297 nm, and emission was monitored at 336 nm. The ratio of melittin/total lipid was 1:200 (mol/mol) and the concentration of melittin was 8.53 μM in all cases. Mean lifetimes were calculated from Table 2 using Eq. 3. See Materials and Methods for other details.

TABLE 3 Acrylamide quenching of tryptophan fluorescence of membrane-bound melittin

Cholesterol* (mol%)	K_{SV}† (M^{-1})	k_q ($\times 10^{-9}$)‡ (M^{-1} s^{-1})
0	2.1 ± 0.15	1.28
20	2.4 ± 0.27	1.54
40	3.3 ± 0.10	2.48

*The ratio of melittin/total lipid was 1:200 (mol/mol) and the concentration of melittin was 1.07 μM in all cases.
†Calculated using Eq. 5. The quenching parameter represents mean ± SE of at least three independent measurements. See Materials and Methods for other details.
‡Calculated using mean fluorescence lifetimes from Table 2 and using Eq. 5. See Materials and Methods for other details.

K_{SV} value of melittin in DOPC vesicles was found to be 2.1 M^{-1}. Incorporation of cholesterol to DOPC vesicles leads to an apparent increase in the accessibility of the melittin tryptophan as evident from an increase in K_{SV} (see Table 3). This suggests that the tryptophan residue in membrane-bound melittin is more exposed (relatively shallow) in membranes containing cholesterol. However, interpretation of K_{SV} values is complicated this way due to its intrinsic dependence on fluorescence lifetime (see Eq. 5). The bimolecular quenching constant (k_q) is therefore a more accurate measure of the degree of exposure because it takes into account the differences in fluorescence lifetime. The k_q values, calculated using mean fluorescence lifetimes from Fig. 5 and Eq. 5, are shown in Table 3. The k_q values are in overall agreement with K_{SV} values implying that the conclusions derived by the analysis of Stern-Volmer constants are not influenced by changes in lifetime. The reason for higher accessibility of the tryptophan in membranes containing cholesterol could be due to increased permeability to small molecules by cholesterol (as shown above by increased water penetration). In addition, increased accessibility could also be due to any change in the tryptophan location (depth) in membranes containing cholesterol. Analysis of membrane penetration depth confirms the latter possibility (see below).

Cholesterol influences tryptophan depth in membrane-bound melittin

Membrane penetration depth represents an important parameter in the study of membrane structure and organization (Chattopadhyay, 1992; London and Ladokhin, 2002). Knowledge of the precise depth of a membrane-embedded group or molecule often helps define the conformation and topology of membrane probes and proteins. In addition, properties such as polarity, fluidity, segmental motion, ability to form hydrogen bonds, and the extent of solvent penetration are known to vary in a depth-dependent manner in the membrane. To gain a better understanding of the organization and conformation of membrane-bound melittin in the presence of cholesterol, penetration depths of the sole tryptophan residue of melittin in membranes were determined. Depth of the tryptophan residue was calculated by the parallax method (Chattopadhyay and London, 1987) using the equation:

$$z_{cF} = L_{c1} + \{[(-1/\pi C)\ln(F_1/F_2) - L_{21}^2]/2L_{21}\}, \quad (10)$$

where z_{cF} = the depth of the fluorophore from the center of the bilayer, L_{c1} = the distance of the center of the bilayer from the shallow quencher (5-PC in this case), L_{21} = the difference in depth between the two quenchers (i.e., the transverse distance between the shallow and the deep quencher), and C = the two-dimensional quencher concentration in the plane of the membrane (molecules/Å^2). Here F_1/F_2 is the ratio of F_1/F_o and F_2/F_o in which F_1 and F_2 are fluorescence intensities in the presence of the shallow (5-PC) and deep quencher (12-PC), respectively, both at the same quencher concentration C; F_o is the fluorescence intensity in the absence of any quencher. All the bilayer parameters used were the same as described previously (Chattopadhyay and London, 1987). The depths of penetration of the tryptophan residue for melittin bound to DOPC vesicles containing varying amounts of cholesterol are shown in Table 4. The depth of penetration of the tryptophan residue for melittin bound to DOPC vesicles is found to be 10.6 Å from the center of the bilayer, in agreement with our previous results (Ghosh et al., 1997), and with the value determined by fluorescence quenching using brominated phospholipids and the distribution analysis method (Ladokhin and Holloway, 1995). Interestingly, the depth of penetration of the tryptophan residue of membrane-bound melittin changes to 17.4 and 18.2 Å in DOPC vesicles containing 20 and 40 mol% cholesterol, respectively (see Table 4). This indicates that the tryptophan is localized at a relatively shallow depth in membranes containing cholesterol. This observation is consistent with the relatively red-shifted fluorescence emission maximum of membrane-bound melittin in the presence of cholesterol (see Table 1) and the acrylamide quenching results (Table 3) in which it was shown that the

TABLE 4 Penetration depth of the tryptophan in membrane-bound melittin by the parallax method

Cholesterol* (mol%)	Distance from the center of the bilayer, z_{cF} (Å)†
0	10.6
20	17.4
40	18.2

*Corrections were made for the altered concentrations of spin-labeled lipids (for lateral distribution) and the depths of the quenchers used in membranes containing cholesterol (Kaiser and London, 1998).
†Depths were calculated from fluorescence quenchings obtained with samples containing 15 mol% of 5-PC and 12-PC and using Eq. 10. Samples were excited at 280 nm, and emission was collected at 336 nm. The ratio of melittin/total lipid was 1:200 (mol/mol) and the concentration of melittin was 2.13 μM in all cases. See Materials and Methods for other details.

tryptophan is more exposed to the aqueous phase in DOPC vesicles containing cholesterol.

In membranes containing cholesterol, the (lateral) concentration of spin-labeled phospholipids and their depths in the membrane are altered. These values were calculated as described previously (Kaiser and London, 1998). It should be mentioned here that the phase properties of 5- and 12-PC are such that no phase separation is expected to be induced when these spin-labeled phospholipids, when used in such small concentrations (15 mol%), are mixed with DOPC at room temperature (Chen and Gaffney, 1978; Ahmed et al., 1997). A minor concern arises from the possibility of partitioning of the spin-labeled phospholipids into cholesterol-rich or -poor regions and its effect on penetration depth. However, this appears to be not a serious concern because it has been previously shown that in the case of a spin-labeled phospholipid (12-PC) incorporated in a mixture of DOPC and cholesterol, the membrane behaves as a single-phase mixture that rules out any specific partitioning of spin-labeled phospholipids into cholesterol-rich or cholesterol-poor domains (Ahmed et al., 1997).

Secondary structure of membrane-bound melittin

To investigate the effect of cholesterol on the secondary structure of melittin, we carried out far-UV CD spectroscopy of melittin in membranes containing various amounts of cholesterol. It is well established that monomeric melittin in aqueous solution shows essentially random coil conformation as reported earlier (Ghosh et al., 1997). On the other hand, membrane-bound melittin shows a CD spectrum that is characteristic of an α-helical conformation (Ghosh et al., 1997; Yang et al., 2001). The CD spectra of melittin in buffer and when bound to membranes composed of varying concentrations of cholesterol are shown in Fig. 6. Our results show that the secondary structure of membrane-bound melittin does not appear to be sensitive to the presence of membrane cholesterol.

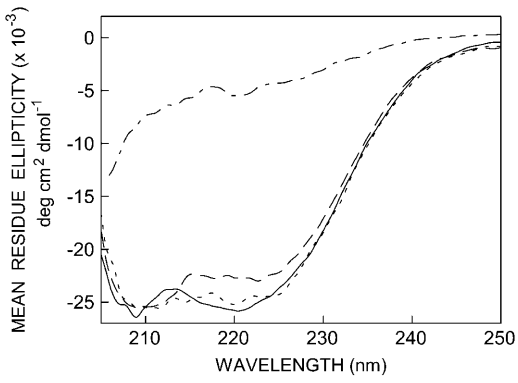

FIGURE 6 Far-UV CD spectra of melittin in buffer (*dashed-dotted line*), and in DOPC vesicles containing 0 (*dashed line*), 20 (*dotted line*), and 40 (*solid line*) mol% cholesterol. The ratio of melittin/total lipid was 1:100 (mol/mol) and the concentration of melittin was 17.1 μM in all cases. See Materials and Methods for other details.

Interaction of melittin with membrane cholesterol: resonance energy transfer with dehydroergosterol

To explore whether there is any specific interaction of melittin with membrane cholesterol, we utilized energy transfer measurements using melittin tryptophan as the donor and dehydroergosterol (DHE) as acceptor. DHE is a naturally occurring fluorescent analog of cholesterol that is found in yeast and differs from cholesterol in having three additional double bonds and a methyl group. A number of reports have shown that DHE faithfully mimics natural cholesterol in biophysical, biochemical, and cell biological studies (Schroeder et al., 1991; Mukherjee et al., 1998). For example, up to 85% of the endogeneous sterol in cultured fibroblast cells could be replaced with DHE with no significant effect on growth property, membrane composition, or activities of membrane enzymes (Schroeder et al., 1991).

Fig. 7 *a* shows that there is substantial spectral overlap between the emission spectrum of membrane-bound melittin tryptophan with the absorption spectrum of membrane-bound DHE, which is an essential criterion for efficient energy transfer. This makes melittin and DHE a good donor and acceptor pair for energy transfer experiments. The distance (in Å) between the donor and acceptor (R_o) that results in 50% energy transfer efficiency can be calculated using the equation (Lakowicz, 1999):

$$R_o = 9.79 \times 10^3 (J\kappa^2 n^{-4})^{1/6}, \tag{11}$$

where J is the spectral overlap integral (in $M^{-1}cm^3$) between the emission spectrum of the donor and the absorption spectrum of the acceptor, κ^2 is the dipole-dipole orientation factor for the donor and acceptor, Q_D is the quantum yield of the donor in the absence of acceptor, and n is the refractive index of the medium. The fluorescence quantum yield (Q_D) of membrane-bound melittin was determined to be 0.06. J was determined from the fluorescence emission of melittin and the absorption of DHE (Fig. 7 *a*) by using the equation (Lakowicz, 1999):

$$J = \int_o^\infty F_D(\lambda)\varepsilon_A(\lambda)\lambda^4 d\lambda, \tag{12}$$

where $F_D(\lambda)$ is the fractional fluorescence intensity of the donor at wavelength λ, $\varepsilon_A(\lambda)$ is the molar extinction coefficient of the acceptor at wavelength λ. The value of J was calculated using a previously written program (Kumar and Chatterji, 1990) and was found to be 2.3×10^{-15} $M^{-1}cm^3$. The value of κ^2, which is a function of the relative orientation of donor emission and acceptor absorption

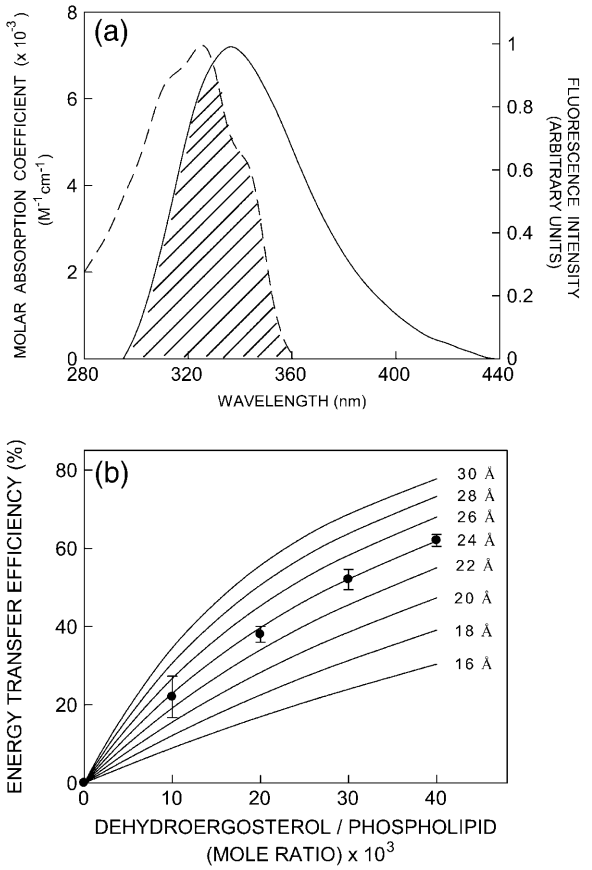

FIGURE 7 (*a*) Spectral overlap (shown as *striped area*) between the corrected fluorescence emission spectrum of melittin (*solid line*) and the absorption spectrum of DHE (*dashed line*) in DOPC vesicles. The excitation wavelength used for melittin was 280 nm. See Materials and Methods for other details. (*b*) Efficiency of energy transfer from melittin to DHE as a function of DHE/phospholipid ratio. The figure shows a series of theoretical plots (*solid lines*) of energy transfer at various acceptor densities in the membrane bilayer for pairs of donors and acceptors with varying R_o ($R_o = 16$–30 Å) assuming random distribution of donors and acceptors in the plane of the bilayer. These plots were generated according to the formalism developed by Fung and Stryer (1978). The experimentally determined energy transfer efficiencies for melittin/DHE pair (●), calculated from tryptophan (donor) quenching (by DHE) using Eq. 6, are superimposed on the theoretical plots. R_o for the melittin/DHE pair was calculated to be 16 Å (see Results). An R_o value of 24 Å gave the best fit to the experimental data. The measured efficiency of energy transfer thus substantially exceeded the calculated value of R_o (16 Å). The donor (melittin) concentration was fixed at 1 mol% of the total amount of lipid used, which corresponds to a ratio of 1:100 (mol/mol) melittin/total lipid (DOPC and DHE). Acceptor density was varied from 0 to 4 mol% of the total lipid used. Excitation wavelength used was 280 nm and emission was collected at 336 nm. See Materials and Methods for other details.

moments, was assumed to be 2/3, the dynamic average of random orientation of the donor and acceptor. This value of κ^2 implies that there is rapid, isotropic reorientation of the donor and acceptor moments during the donor emission lifetime. This assumption could be rationalized for membrane-bound donors and acceptors (Estep and Thompson, 1979). R_o for melittin-DHE pair was calculated using Eq. 11 and was found to be 16.0 Å. Because the melittin tryptophan is localized at the interfacial region of the membrane, this value of R_o ensures that there is no vertical energy transfer from one leaflet to another (Fung and Stryer, 1978).

The extent of energy transfer can be quantitated by determining the extent of tryptophan quenching. The dependence of efficiency of energy transfer on surface densities of the acceptor (DHE) for various R_o is shown in Fig. 7 *b*. The experimentally obtained energy transfer efficiencies were then compared with calculated efficiencies of energy transfer for a random distribution of donors and acceptors in a two dimensional plane using the formalism developed by Fung and Stryer (1978). The series of theoretical plots of energy transfer efficiency versus acceptor surface density in the membrane, for pairs of donors and acceptors with varying R_o and randomly distributed in the plane of the bilayer, were generated by numerical integration of the equation (Fung and Stryer, 1978):

$$E = 1 - (1/\tau_o)\int_o^\infty [F(t)/F(0)]dt, \tag{13}$$

where τ_o is the excited-state lifetime of the donor in the absence of acceptor, and $F(t)$ is the fluorescence intensity of the donor in an infinite plane at time t and is given by

$$F(t) = F(0)e^{-t/\tau o}e^{-\sigma S(t)}, \tag{14}$$

where $e^{-\sigma\, S(t)}$ is the energy transfer term, $F(0)$ is the initial fluorescence intensity, σ is the surface density of the acceptor (acceptor per phospholipid assuming the area occupied by a phospholipid molecule is 70 Å^2), and $S(t)$ is given by

$$S(t) = \int_a^\infty [1 - e^{-(t/\tau o)(Ro/r)6}]\, 2\pi r dr, \tag{15}$$

where a is the distance of closest approach of donor and acceptor (9.9 Å for melittin-DHE pair), and the expression $2\pi r dr$ represents the probability of finding an acceptor within a distance r from the donor in two dimensions and R_o is the distance (in Å) between the donor and acceptor at which 50% energy transfer takes place. The dependence of energy transfer efficiency on the surface density of the acceptor for values of R_o ranging from 16 to 30 Å, calculated by numerical integration of Eqs. 14 and 15 and assuming random distribution of donors and acceptors in the plane of the bilayer (Fung and Stryer, 1978), is shown in Fig. 7 *b*. The experimental data points were superimposed on the theoretical curves and the experimental data fitted best to a R_o of 24 Å. The measured efficiency of energy transfer thus substantially exceeded the calculated value of R_o (16.0 Å). This would be expected if there is a preferential association of the donor and acceptor in the membrane (Lakowicz, 1999).

These results therefore suggest that there is a close molecular interaction between melittin and dehydroergosterol at low sterol concentrations.

DISCUSSION

Lipid-protein interactions are vital for the organization and function of biological membranes (Lee, 2003). Study of lipid-protein interactions is of particular importance because a cell has the ability of varying the lipid composition of its membrane in response to a variety of stress and stimuli, thus changing the environment and the activity of the proteins in its membrane. Cholesterol is a ubiquitous membrane component of eukaryotic organisms (Bloch, 1983) and has been reported to be necessary for the functional activity of many membrane proteins and receptors (Yeagle, 1985; Gimpl et al., 1997; Pucadyil and Chattopadhyay, 2004). Cholesterol affects the physical properties of model and biological membranes (Yeagle, 1985). In addition, it increases the order of the acyl chains in fluid membranes and as a consequence, leads to tighter acyl chain packing, a thicker bilayer, and reduced lipid surface area (Yeagle, 1985; Nezil and Bloom, 1992).

The distribution of cholesterol in the membranes of the cellular organelles is not uniform and the cholesterol content in eukaryotic plasma membranes is usually rather high (e.g., ~45 mol% in human erythrocytes) whereas the internal organelle membranes have much less amounts of cholesterol (Yeagle, 1985). Cholesterol is often laterally associated with sphingolipids in plasma membranes to form lateral membrane heterogeneities called membrane microdomains or rafts that have been implicated in membrane traffic and cell signaling in mammalian cells (Simons and Ikonen, 1997, 2000). In view of the importance of the cholesterol in relation to membrane domains, the interaction of cholesterol with membrane proteins and peptides assumes significance with respect to their organization and function. Interestingly, these microdomains act as concentration platforms to facilitate entry of pore-forming toxins (Abrami and van der Goot, 1999). In addition, it has been proposed that cholesterol could act as a target for many pore-forming toxins (de Kruijff, 1990).

In this article, we have monitored the organization and dynamics of the hemolytic peptide melittin in membranes containing cholesterol by utilizing the intrinsic fluorescence properties of its functionally important sole tryptophan residue and CD spectroscopy. The significance of this study is based on the fact that the natural target for melittin is the erythrocyte membrane that contains high amounts of cholesterol. Our results show that the presence of cholesterol inhibits melittin-induced leakage of lipid vesicles and the extent of inhibition appears to be dependent on the concentration of membrane cholesterol. A similar inhibition by cholesterol has been reported for melittin-induced leakage from POPC vesicles (Benachir et al., 1997). In addition, cholesterol has been shown to inhibit the lytic activity of mastoparan, a wasp venom toxin with a strong structural resemblance to melittin (Katsu et al., 1990), and *Gardnerella vaginalis* cytolysin (Cauci et al., 1993). Tight lipid packing and increased deformation energy (see later) induced by cholesterol could account for such effects. Further, our results show that the presence of increasing amounts of cholesterol strongly reduces the binding of melittin to the lipid vesicles, i.e., threefold excess lipid is needed in order for melittin to be completely bound to DOPC membranes in the presence of cholesterol (Fig. 2). The reduced lytic effect of melittin in the presence of cholesterol could also be due to reduced binding of the peptide to the bilayer.

We show here that fluorescence parameters such as intensity, emission maximum, and lifetime of membrane-bound melittin indicate a change in polarity in the immediate vicinity of the tryptophan probably due to increased water penetration in the presence of cholesterol. This is supported by results from fluorescence quenching experiments using acrylamide as the quencher. Tryptophan penetration depths for membrane-bound melittin were analyzed by the parallax method. Because melittin has a single tryptophan, the interpretation of depth values obtained is devoid of complications that often arise from depth analysis of multi tryptophan proteins. Our results show that the depth of penetration of the tryptophan residue for melittin bound to DOPC vesicles to be 10.6 Å from the center of the bilayer. The depth of penetration of the tryptophan residue of membrane-bound melittin changes to 17.4 and 18.2 Å in DOPC vesicles containing 20 and 40 mol% cholesterol suggesting that the tryptophan is localized at a relatively shallow depth in membranes containing cholesterol (see Fig. 8). Similar reduction in the depth of penetration has been reported for peptides such as temporin L (Zhao and Kinnunen, 2002) and amphipathic class A peptide (Gorbenko et al., 2003). This is probably due to the increase in elastic modulus (and hence increase in bilayer deformation energy) by several folds in the presence of high amounts of cholesterol (Needham, 1995).

We carried out resonance energy transfer experiments using DHE and melittin to investigate the possibility of specific interaction of melittin with cholesterol. Analysis of energy transfer results indicates that DHE is not randomly distributed in the membrane and is rather preferentially localized around the tryptophan residue of membrane-bound melittin, even at the low concentrations used (1–4 mol%). Because DHE is a naturally occurring fluorescent cholesterol analog that has been shown to faithfully mimic cholesterol, we interpret this result as specific interaction of melittin with membrane cholesterol (Fig. 8). Interestingly, it has been shown earlier by us (Mukherjee and Chattopadhyay, 1996; Rukmini et al., 2001) and others (Loura and Prieto, 1997) that both cholesterol and DHE can exhibit local order and organization even at such low concentrations.

The existence of membrane domains in human erythrocytes has previously been reported. Although the exact nature of these domains is not still resolved, high amounts of

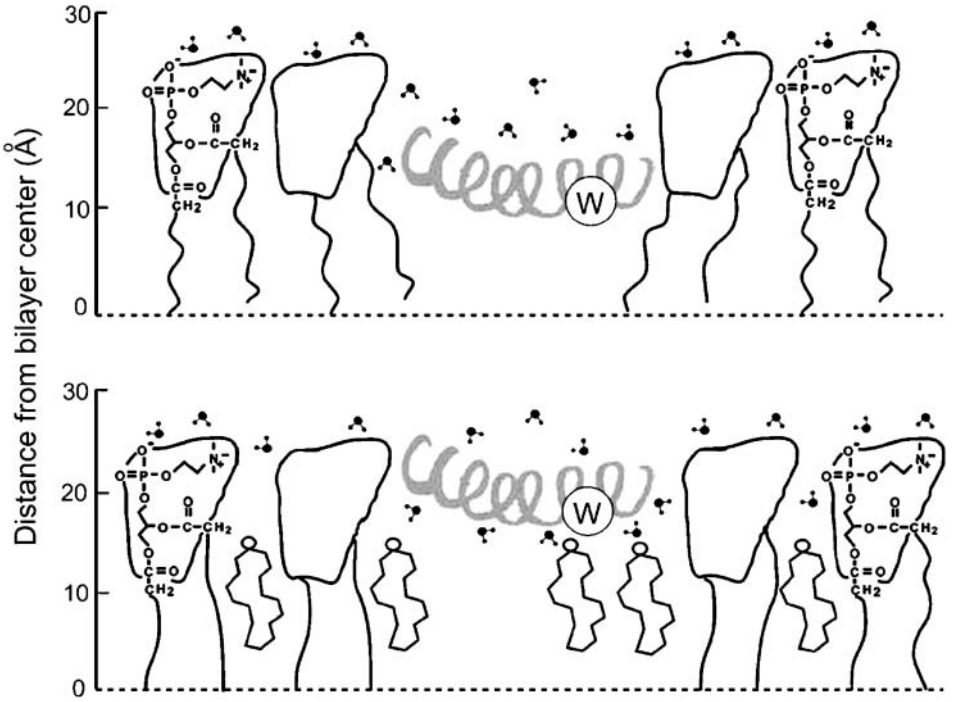

FIGURE 8 A schematic representation of the membrane bilayer showing the orientation and location of membrane-bound melittin in the absence (*top*) and presence (*bottom*) of cholesterol. The small v-shaped structures represent membrane associated water molecules. The sole tryptophan residue (W) of melittin is shown to be localized in the interfacial region of membranes in both cases. However, melittin tryptophan is localized at a relatively shallow depth in membranes containing cholesterol (Table 4). The specific interaction of melittin with membrane cholesterol is shown as a cluster of cholesterol around melittin tryptophan (Fig. 7 *b*). In addition, the global bilayer effect of cholesterol is indicated by a change in headgroup packing and an increase in water penetration in the immediate vicinity of the tryptophan residue. The dotted line indicates the center of the bilayer. See text for other details.

cholesterol in the erythrocyte membrane could induce raft-like membrane microdomains (Samuel et al., 2001), which may have sphingolipids as the other lipid component. The distribution of lipids in the erythrocyte membrane therefore is not homogenous. The fact that cholesterol inhibits the lytic activity of melittin, whose target is the erythrocyte membrane with high amounts of cholesterol, raises an interesting scenario. It is interesting to note that the interaction of another hemolytic protein, the earthworm hemolysin eiseniapore, with lipid membranes has been shown to require sphingolipids (Lange et al., 1997). Interestingly, the presence of cholesterol enhances the hemolytic activity of eiseniapore toward sphingomyelin-containing vesicles probably due to its specific interaction with sphingomyelin. In addition, it has been recently shown that cholesterol, along with cone-shaped lipids, increases membrane permeabilization by the cholesterol-specific cytolysins (Zitzer et al., 2001). However, the membrane permeabilization is inefficient if only sterol is present. Although our study shows that cholesterol inhibits the lytic activity of melittin, the possibility of preferential localization of melittin in cholesterol-sphingolipid-rich domains cannot be ruled out because cholesterol-sphingolipid-rich plasma membrane microdomains (rafts) have been reported to act as concentration platforms for pore-forming toxins (Abrami and van der Goot, 1999). It is also interesting to note that the Nef protein of HIV-1, whose N-terminal region (Nef1-25) resembles melittin (Barnham et al., 1997), has been shown to associate with membrane rafts for its activity (Wang et al., 2000). Whether melittin requires a similar association with raft-like domains in erythrocytes represents an exciting possibility. We plan to address this issue in future studies in our laboratory. In summary, our results are relevant in understanding the interaction of melittin with membranes in general, and with cholesterol-containing membranes in particular.

We sincerely thank Professor Dipankar Chatterji and A. Sharada Devi for help with the program used for calculation of the spectral overlap integral, and Dr. Somdatta Sinha for help with the program used for simulation of energy transfer efficiencies using numerical integration. We gratefully acknowledge R. Rukmini for help with the membrane penetration depth experiments. We thank Dr. R. Nagaraj and C. Subbalakshmi for help with the membrane permeabilization assay, and Y. S. S. V. Prasad and G. G. Kingi for technical help. We express our thanks and appreciation to Devaki Kelkar, Shanti Kalipatnapu, and Thomas Pucadyil for reading the manuscript critically and for providing useful comments.

This work was supported by the Council of Scientific and Industrial Research, Government of India. H. R. thanks the University Grants Commission, Government of India, for the award of a Senior Research Fellowship.

REFERENCES

Abrami, L., and F. G. van der Goot. 1999. Plasma membrane microdomains act as concentration platforms to facilitate intoxication by aerolysin. *J. Cell Biol.* 147:175–184.

Abrams, F. S., and E. London. 1993. Extension of the parallax analysis of membrane penetration depth to the polar region of model membranes: use of fluorescence quenching by a spin-label attached to the phospholipid polar headgroup. *Biochemistry.* 32:10826–10831.

Ahmed, S. N., D. A. Brown, and E. London. 1997. On the origin of sphingolipid/cholesterol-rich detergent-insoluble cell membranes: physiological concentrations of cholesterol and sphingolipid induce formation of detergent-insoluble, liquid-ordered lipid phase in model membranes. *Biochemistry.* 36:10944–10953.

Allen, T. M. 1984. Calcein as a tool in liposome methodology. *In* Liposome Technology. G. Gregoriadis, editor. CRC Press, Boca Raton, FL. 177–182.

Barnham, K. J., S. A. Monks, M. G. Hinds, A. A. Azad, and R. S. Norton. 1997. Solution structure of polypeptide from the N terminus of the HIV protein Nef. *Biochemistry.* 36:5970–5980.

Benachir, T., M. Monette, J. Grenier, and M. Lafleur. 1997. Melittin-induced leakage from phosphatidylcholine vesicles is modulated by cholesterol: a property used for membrane targeting. *Eur. Biophys. J.* 25:201–210.

Bloch, K. E. 1983. Sterol structure and membrane function. *Crit. Rev. Biochem.* 14:47–92.

Blondelle, S. E., and R. A. Houghten. 1991a. Probing the relationships between the structure and hemolytic activity of melittin with a complete set of leucine substitution analogues. *Pept. Res.* 4:12–18.

Blondelle, S. E., and R. A. Houghten. 1991b. Hemolytic and antimicrobial activities of twenty-four individual omission analogues of melittin. *Biochemistry.* 30:4671–4678.

Bradrick, T. D., A. Philippetis, and S. Georghiou. 1995. Stopped-flow fluorometric study of the interaction of melittin with phospholipid bilayers: importance of the physical state of the bilayer and the acyl chain length. *Biophys. J.* 69:1999–2010.

Cauci, S., R. Monte, M. Ropele, C. Missero, T. Not, F. Quadrifoglio, and G. Menestrina. 1993. Pore-forming and haemolytic properties of the *Gardnerella vaginalis* cytolysin. *Mol. Microbiol.* 9:1143–1155.

Chattopadhyay, A. 1992. Membrane penetration depth analysis using fluorescence quenching: a critical review. *In* Biomembrane Structure and Function: The State of the Art. B. P. Gaber and K. R. K. Easwaran, editors. Adenine Press, Schenectady, NY. 153–163.

Chattopadhyay, A. 2003. Exploring membrane organization and dynamics by the wavelength-selective fluorescence approach. *Chem. Phys. Lipids.* 122:3–17.

Chattopadhyay, A., and E. London. 1987. Parallax method for direct measurement of membrane penetration depth utilizing fluorescence quenching by spin-labeled phospholipids. *Biochemistry.* 26:39–45.

Chattopadhyay, A., S. Mukherjee, R. Rukmini, S. S. Rawat, and S. Sudha. 1997. Ionization, partitioning, and dynamics of tryptophan octyl ester: implications for membrane-bound tryptophan residues. *Biophys. J.* 73: 839–849.

Chattopadhyay, A., and R. Rukmini. 1993. Restricted mobility of the sole tryptophan in membrane-bound melittin. *FEBS Lett.* 335:341–344.

Chen, S.-C., and B. J. Gaffney. 1978. Paramagnetic resonance evidence for phase transitions in bilayers of pure spin-labeled lipids. *J. Mag. Res.* 29: 341–353.

de Kruijff, B. 1990. Cholesterol as a target for toxins. *Biosci. Rep.* 10: 127–130.

Demchenko, A. P. 2002. The red-edge effects: 30 years of exploration. *Luminescence.* 17:19–42.

Dempsey, C. E. 1990. The actions of melittin on membranes. *Biochim. Biophys. Acta.* 1031:143–161.

Dittmer, J. C., and R. L. Lester. 1964. Simple, specific spray for the detection of phospholipids on the thin-layer chromatograms. *J. Lipid Res.* 5:126–127.

Eftink, M. R. 1991a. Fluorescence quenching reactions: probing biological macromolecular structure. *In* Biophysical and Biochemical Aspects of Fluorescence Spectroscopy. T. G. Dewey, editor. Plenum Press, New York. 1–41.

Eftink, M. R. 1991b. Fluorescence quenching: theory and applications. *In* Topics in Fluorescence Spectroscopy, Vol. 2. J. R. Lakowicz, editor. Plenum Press, New York. 53–126.

Estep, T. N., and T. E. Thompson. 1979. Energy transfer in lipid bilayers. *Biophys. J.* 26:195–207.

Fung, L. K., and L. Stryer. 1978. Surface density determination in membranes by fluorescence energy transfer. *Biochemistry.* 17:5241–5248.

Ghosh, A. K., R. Rukmini, and A. Chattopadhyay. 1997. Modulation of tryptophan environment in membrane-bound melittin by negatively charged phospholipids: implications in membrane organization and function. *Biochemistry.* 36:14291–14305.

Gimpl, G., K. Burger, and F. Fahrenholz. 1997. Cholesterol as modulator of receptor function. *Biochemistry.* 36:10959–10974.

Golding, C., and P. O'Shea. 1995. The interactions of signal sequences with membranes. *Biochem. Soc. Trans.* 23:971–976.

Gorbenko, G., T. Handa, H. Saito, J. Molotkovsky, M. Tanaka, M. Egashira, and M. Nakano. 2003. Effect of cholesterol on bilayer location of the class A peptide Ac-18A-NH_2 as revealed by fluorescence resonance energy transfer. *Eur. Biophys. J.* 32:703–709.

Habermann, E., and H. Kowallek. 1970. Modifications of amino groups and tryptophan in melittin as an aid to recognition of structure-activity relationships. *Hoppe-Seyler's Z. Physiol. Chem.* 351:884–890.

Kaiser, R. D., and E. London. 1998. Location of diphenylhexatriene (DPH) and its derivatives within membranes: comparison of different fluorescence quenching analyses of membrane depth. *Biochemistry.* 37:8180–8190.

Katsu, T., M. Kuroko, T. Morikawa, K. Sanchika, H. Yamanaka, S. Shinoda, and Y. Fujita. 1990. Interaction of wasp venom mastoparan with biomembranes. *Biochim. Biophys. Acta.* 1027:185–190.

Kelkar, D. A., A. Ghosh, and A. Chattopadhyay. 2003. Modulation of fluorophore environment in host membranes of varying charge. *J. Fluoresc.* 13:459–466.

Kirby, E. P., and R. F. Steiner. 1970. The influence of solvent and temperature upon the fluorescence of indole derivatives. *J. Phys. Chem.* 74:4480–4490.

Kremer, J. M. H., M. W. van der Esker, C. Pathmamanoharan, and P. H. Wiersema. 1977. Vesicles of variable diameter prepared by a modified injection method. *Biochemistry.* 16:3932–3935.

Kumar, K. P., and D. Chatterji. 1990. Resonance energy transfer study on the proximity relationship between the GTP binding site and the rifampicin binding site of *Escherichia coli* RNA polymerase. *Biochemistry.* 29:317–322.

Ladokhin, A. S. 2000. Fluorescence spectroscopy in peptide and protein analysis. *In* Encyclopedia of Analytical Chemistry. R. A. Meyers, editor. John Wiley, Chichester, UK. 5762–5779.

Ladokhin, A. S., and P. W. Holloway. 1995. Fluorescence of membrane-bound tryptophan octyl ester: a model for studying intrinsic fluorescence of protein-membrane interactions. *Biophys. J.* 69:506–517.

Lakowicz, J. R. 1999. Principles of fluorescence spectroscopy. Kluwer-Plenum, New York.

Lange, S., F. Nussler, E. Kauschke, G. Lutsch, E. L. Cooper, and A. Herrmann. 1997. Interaction of earthworm hemolysin with lipid membranes requires sphingolipids. *J. Biol. Chem.* 272:20884–20892.

Lee, A. G. 2003. Lipid-protein interactions in biological membranes: a structural perspective. *Biochim. Biophys. Acta.* 1612:1–40.

London, E., and A. S. Ladokhin. 2002. Measuring the depth of amino acid residues in membrane-inserted peptides by fluorescence quenching. *In* Current Topics in Membranes. D. Benos, and S. Simon, editors. Elsevier, San Diego, CA. 89–115.

Loura, L. M. S., and M. Prieto. 1997. Dehydroergosterol structural organization in aqueous medium and in a model system of membranes. *Biophys. J.* 72:2226–2236.

McClare, C. W. F. 1971. An accurate and convenient organic phosphorus assay. *Anal. Biochem.* 39:527–530.

Mukherjee, S., and A. Chattopadhyay. 1995. Wavelength-selective fluorescence as a novel tool to study organization and dynamics in complex biological systems. *J. Fluoresc.* 5:237–246.

Mukherjee, S., and A. Chattopadhyay. 1996. Membrane organization at low cholesterol concentrations: a study using 7-nitrobenz-2-oxa-1,3-diazol-4-yl-labeled cholesterol. *Biochemistry.* 35:1311–1322.

Mukherjee, S., H. Raghuraman, S. Dasgupta, and A. Chattopadhyay. 2004. Organization and dynamics of *N*-(7-nitrobenz-2-oxa-1,3-diazol-4-yl)-labeled lipids: a fluorescence approach. *Chem. Phys. Lipids.* 127:91–101.

Mukherjee, S., X. Zha, I. Tabas, and F. R. Maxfield. 1998. Cholesterol distribution in living cells: fluorescence imaging using dehydroergosterol as a fluorescent cholesterol analog. *Biophys. J.* 75:1915–1925.

Munro, S. 2003. Lipid rafts: elusive or illusive? *Cell.* 115:377–388.

Needham, D. 1995. Cohesion and permeability in lipid bilayer vesicles. *In* Permeability and Stability of Bilayers. S. A. Simon and E. A. Disalvo, editors. CRC Press, Boca Raton, FA. 49–76.

Nezil, F. A., and N. Bloom. 1992. Combined influence of cholesterol and synthetic amphiphilic peptides upon bilayer thickness in model membranes. *Biophys. J.* 61:1176–1183.

Parker, C. A., and W. T. Rees. 1960. Correction of fluorescence spectra and measurement of fluorescence quantum efficiency. *Analyst.* 85:587–600.

Pucadyil, T. J., and A. Chattopadhyay. 2004. Cholesterol modulates ligand binding and G-protein coupling to serotonin$_{1A}$ receptors from bovine hippocampus. *Biochim. Biophys. Acta.* 1663:188–200.

Rabenstein, M., and Y. K. Shin. 1995. A peptide from the heptad repeat of human immunodeficiency virus gp41 shows both membrane binding and coiled-coil formation. *Biochemistry.* 34:13390–13397.

Raghuraman, H., and A. Chattopadhyay. 2003. Organization and dynamics of melittin in environments of graded hydration: a fluorescence approach. *Langmuir.* 19:10332–10341.

Raghuraman, H., and A. Chattopadhyay. 2004. Effect of micellar charge on the conformation and dynamics of melittin. *Eur. Biophys. J.* PMID: 15071759.

Raghuraman, H., D. A. Kelkar, and A. Chattopadhyay. 2003. Novel insights into membrane protein structure and dynamics utilizing the wavelength-selective fluorescence approach. *Proc. Ind. Natl. Sci. Acad. A* 69:25–35.

Raghuraman, H., S. K. Pradhan, and A. Chattopadhyay. 2004. Effect of urea on the organization and dynamics of Triton X-100 micelles: a fluorescence approach. *J. Phys. Chem. B.* 108:2489–2496.

Rawat, S. S., D. A. Kelkar, and A. Chattopadhyay. 2004. Monitoring gramicidin conformations in membranes: a fluorescence approach. *Biophys. J.* 87:831–843.

Rukmini, R., S. S. Rawat, S. C. Biswas, and A. Chattopadhyay. 2001. Cholesterol organization in membranes at low concentrations: effects of curvature stress and membrane thickness. *Biophys. J.* 81:2122–2134.

Saberwal, G., and R. Nagaraj. 1994. Cell-lytic and antibacterial peptides that act by perturbing the barrier function of membranes: facets of their conformational features, structure-function correlation and membrane-perturbing abilities. *Biochim. Biophys. Acta.* 1197:109–131.

Samuel, B. U., N. Mohandas, T. Harrison, H. McManus, W. Rosse, M. Reid, and K. Haldar. 2001. The role of cholesterol and glycosylphosphatidylinositol-anchored proteins of erythrocyte rafts in regulating raft protein content and malarial infection. *J. Biol. Chem.* 276:29319–29329.

Schroeder, F., J. R. Jefferson, A. B. Kier, J. Knittel, T. J. Scallen, W. G. Wood, and I. Hapala. 1991. Membrane cholesterol dynamics: cholesterol domains and kinetic pools. *Proc. Soc. Exp. Biol. Med.* 196:235–252.

Simons, K., and E. Ikonen. 1997. Functional rafts in cell membranes. *Nature.* 387:569–572.

Simons, K., and E. Ikonen. 2000. How cells handle cholesterol. *Science.* 290:1721–1726.

Stewart, J. C. M. 1980. Colorimetric determination of phospholipids with ammonium ferrothiocyanate. *Anal. Biochem.* 104:10–14.

Stubbs, C. D., C. Ho, and S. J. Slater. 1995. Fluorescence techniques for probing water penetration into lipid bilayers. *J. Fluoresc.* 5:19–28.

Subczynski, W. K., A. Wisniewska, J.-J. Yin, J. S. Hyde, and A. Kusumi. 1994. Hydrophobic barriers of lipid bilayer membranes formed by reduction of water penetration by alkyl chain unsaturation and cholesterol. *Biochemistry.* 33:7670–7681.

Szabo, A. G., and D. M. Rayner. 1980. Fluorescence decay of tryptophan conformers in aqueous solution. *J. Am. Chem. Soc.* 102:554–563.

Terwilliger, T. C., and D. Eisenberg. 1982. The structure of melittin. *J. Biol. Chem.* 237:6016–6022.

Wang, J. K., E. Kiyokawa, E. Verdin, and D. Trono. 2000. The Nef protein of HIV-1 associates with rafts and primes T cells for activation. *Proc. Natl. Acad. Sci. USA.* 97:394–399.

Yang, L., T. A. Harroun, T. M. Weiss, L. Ding, and H. W. Huang. 2001. Barrel-stave model or toroidal model? A case study on melittin pores. *Biophys. J.* 81:1475–1485.

Yeagle, P. L. 1985. Cholesterol and the cell membrane. *Biochim. Biophys. Acta.* 822:267–287.

Zhao, H., and P. K. J. Kinnunen. 2002. Binding of the antimicrobial peptide temporin L to liposomes assessed by Trp fluorescence. *J. Biol. Chem.* 277:25170–25177.

Zitzer, A., R. Bittman, C. A. Verbicky, R. K. Erukulla, S. Bhakdi, S. Weis, A. Valeva, and M. Palmer. 2001. Coupling of cholesterol and cone-shaped lipids in bilayers augments membrane permeabilization by the cholesterol-specific toxins streptolysin O and *Vibrio cholerae* cytolysin. *J. Biol. Chem.* 276:14628–14633.